

DESIGN OF A 17.2-MM-PERIOD PLANAR UNDULATOR FOR THE APS *

E.R. Moog[#], M. Abliz, R.J. Dejus, J.H. Grimmer, and M. Jaski, ANL, Argonne, IL 60439, USA

Abstract

The design process for a short-period planar undulator is described. This is a conventional planar design based on Nd-Fe-B magnets and vanadium permendur poles. The period length was driven by the users' request for a high flux of photons at 23.7 keV, with minimal tuning range. A shorter period gives higher flux; 17.2 mm was the shortest value consistent with the gap limitations of the vacuum chamber and with reaching the desired photon energy. Details of the design, especially the various chamfers of edges of the magnet and pole, were examined more closely than has been the standard past practice in order to minimize the period length.

INTRODUCTION

The majority of the insertion devices at the Advanced Photon Source (APS) are of the planar permanent magnet hybrid type, and a variety of period lengths have been installed. This 17.2-mm-period undulator will have the shortest period; it is being designed to meet the specific needs of a group of users who want to maximize their photon flux at 23.7 keV without any need for a significant tuning range. The ideal choice for such a short-period undulator would be to use superconducting technology, but that technology is only now being commissioned at the APS [1]. It will be several years before a customized device can be designed and built for these users. They have opted not to wait.

Keeping the beam impedance from the insertion device vacuum chamber walls low results in a minimum gap for the undulator of 10.4 mm (with a new ID vacuum chamber that is in the design stage; the present typical minimum gap is 11.0 mm). This, combined with the 23.7 keV desired energy, means that the operating point of the undulator is not at the peak in the tuning curve but rather on a slope where a small change in undulator period can have a noticeable effect on the on-axis flux, as shown in Fig. 1 where there is a 15% flux increase between the 17.5 and 17.2-mm period lengths. Shortening the undulator period gives more flux, until the field strength needed to reach the desired energy no longer lies within the achievable gap range. The steepness of the tuning curve for this design project places a high premium on achieving the shortest period possible, and the need for a single specific photon energy means that the magnetic field cannot be lower than expected. To add to the challenge, the required undulator field increases as the undulator period decreases, while a decrease in period generally comes with a decrease in field.

CHOICE OF MAGNET GRADE

The considerations that drive the choice of a magnet grade are the remanent field B_r and the coercivity H_{cJ} of that grade. Recent magnet grades used for APS undulators are Shin-Etsu's N39UH and N42SH. With $B_r \geq 12.7$ kG and $H_{cJ} \geq 21$ kOe, N42SH has been used when the highest field strength was needed. Otherwise, N39UH with $B_r \geq 12.2$ kG and $H_{cJ} \geq 25$ kOe has been chosen for its higher coercivity.

The higher coercivity is desirable for two reasons: 1) for a particular demagnetizing field in the magnet, the higher-coercivity magnet can survive higher temperatures without ill effects, and 2) the higher coercivity correlates with higher resistance to radiation-induced demagnetization. Magnets of either grade, when installed in an undulator whose magnetic design considerations include maintaining a moderate demagnetizing field, will survive a hot day with broken air conditioning. Radiation susceptibility is harder to quantify because of many unknowns, including the spectral sensitivity of the magnets and the spectral distribution of the radiation at the magnets' locations. At the APS, except for two extremely high-dose sectors, the undulators have not been affected by radiation enough to affect users' programs, though small effects have been seen. A common difference between the maximum demagnetizing field and the magnet's H_{cJ} has been ~ 4 kOe, so a goal is to keep the demagnetizing field at least that far below H_{cJ} . For this short a period, a higher H_{cJ} than N42SH is not necessary.

The magnet grade characteristics given here are from the manufacturer's data sheets and are for 20°C. The temperature of the APS storage ring tunnel, however, is 25°C. Since the on-axis field in the simulations must be met in the real device, the reduction in the manufacturer's B_r due to the higher temperature must be taken into

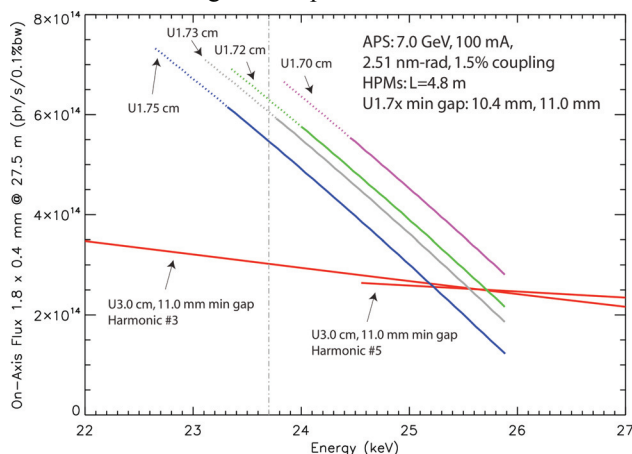


Figure 1: Tuning curves over a narrow photon energy range, for a few period lengths. The solid lines are for a minimum gap of 11 mm; the dotted extensions are for a reduction to 10.4-mm gap.

*Work supported by U.S. Dept. of Energy, Office of Science, under Contract No. DE-AC02-06CH11357.
[#]emoog@aps.anl.gov

account. Thus the B_r used in magnetic design calculations is 12.63 kG, after applying the $-0.11\%/K$ thermal coefficient correction.

DESIGN PROCESS

In order to finalize the period length, a series of quick calculations was carried out to determine approximately what field strength could be obtained from a variety of period lengths. Both 2-D and 3-D modules from the Vector Fields suite of magnetic design codes [2] were used. The only optimization was to ensure that the relative thicknesses of magnet and pole were close to optimal. From these results, a period length of 17.2 mm was chosen (see Fig. 1). The field requirement would be met with the new ID vacuum chamber; it might be met if a gap smaller than 11 mm could be achieved with the present chamber and if the delivered magnets are stronger than the minimum for the magnet grade.

2-D Design Work

Some initial magnetic design tasks can be carried out using the 2-dimensional codes. The calculations are slightly quicker and the optimization of the chamfering was found to be somewhat quieter than in 3-D. The results were later confirmed in 3-D.

The 2-D magnet model is shown in Fig. 2. The entire non-air part of the model is shown along with an inset showing an enlargement of the gap region. (The entire model includes more air on the non-gap side—enough so the boundary condition there doesn't matter.) Symmetry conditions allow just the quarter-period section shown, with only one jaw, to be calculated. Perpendicular axis boundary conditions are applied along the beam axis (i.e., the undulator midplane) and the top boundary, which is the center of the magnet in the beam direction. The lower boundary (the center of the pole) has the magnetic field parallel to the boundary. The pole protrudes into the gap beyond the magnet, leaving a 0.5-mm magnet recess space available for shims to be placed during magnetic tuning of the completed undulator without affecting the minimum undulator gap. This space is needed despite its cost in on-axis field. A small air gap of 0.08 mm is allowed between the magnet and pole, reflecting the

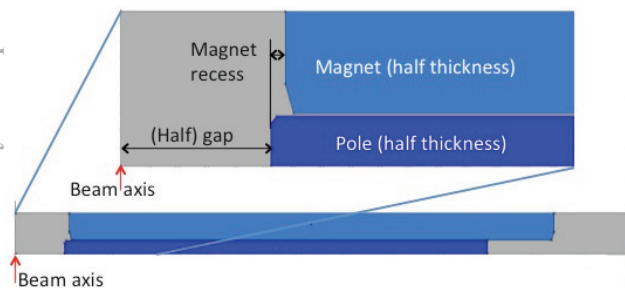


Figure 2: The two-dimensional magnetic model is shown at the bottom, with additional air space at the right omitted. The top section is an enlargement of the gap region, showing the chamfers and the thin air gap between magnet and pole.

tolerance in the magnet and pole dimensions. The chamfers on the corners of the magnet and pole can also be seen.

The goal of the magnetic design is to maximize the on-axis field of the undulator while not allowing the demagnetizing field in the magnet (the H component parallel to the beam axis, since the magnetization direction of the magnet is parallel to the beam axis) to become too large compared to the magnet grade's H_{cJ} .

The field strength is very sensitive to the thickness (in the beam direction) of the magnet and pole, so it is optimized first. It is also rechecked last, once everything else has been set. Model calculations as a function of magnet thickness find an optimum peak field on axis at a magnet thickness of 5.67 mm. The peak field changes by 1 in 1000 at a thickness change of ± 0.047 mm, leading to a tolerance on magnet thickness of ± 0.05 mm. (The final recheck of the magnet thickness resulted in an adjustment to 5.63 mm. The pole thickness then becomes 2.81 mm.)

There isn't an optimum magnet height—a taller magnet will always give more field, albeit with diminishing returns, as long as the pole height is sensible. Therefore, the height chosen for the magnet, 52.5 mm, was the tallest that would fit without any redesign of the strongback or gap separation mechanism and without reducing the maximum achievable gap.

The pole height was adjusted to maximize on-axis field, giving a height of 45 mm. This is a broad maximum—it takes a 3-mm change to change the peak by 1 in 1000.

The remaining parameters to set using the 2-D model are the chamfers. There are four parameters to set: the y (vertical) and z (beam direction) dimensions on both the pole and magnet. An attempt to use the Optimizer module from Vector Fields [2] to set all four parameters at once was unsuccessful, but showed that the largest on-axis field was for the least pole material removed by the chamfering. Following the mechanical engineers' advice that the edges should be broken at least slightly, both pole chamfer dimensions are set to 0.15 mm.

Setting the magnet chamfers involves a trade-off between the on-axis field and the demagnetizing field inside the magnet. The surface plots in Fig. 3 show the behavior of both as a function of the magnet chamfer z dimension, Ch_{zz} , and the magnet chamfer y dimension, Ch_{zy} . (The z in the name is a reminder that this is a chamfer on the edge at the z end of the magnet. The chamfer at the x end will be considered below.) The top panel shows the effective field $B_{y,eff}$ as a function of the chamfer dimensions. A ridge of higher field can be seen, with a sharper drop-off on the right side in the figure. The lower panel shows the worst value of the demagnetizing field in the magnet block, with the value closest to zero being desirable. It too shows a ridge, but one that runs perpendicular to that in the top panel. Originally the red point was chosen, where the two ridges cross. A slightly higher $B_{y,eff}$ (by ~ 1 G) could be reached, but the decision was made to save a few kOe instead. Later, concerns were raised that the zz chamfer was too long to allow shims to be placed stably on the magnet faces, so Ch_{zz} was

reduced to 0.5 mm. This change reduced the field by 0.9 G, a negligible amount, and made $H_{z \max}$ worse by 660 Oe.

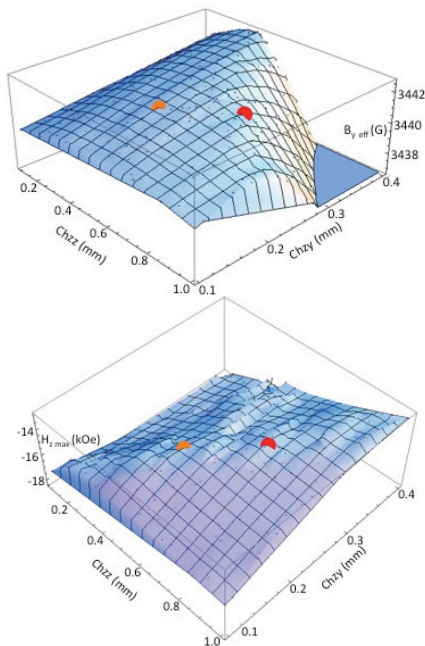


Figure 3: Surface plots showing the dependence of the effective field $B_{y \text{ eff}}$ (top) and the strongest demagnetizing field in the magnet block $H_{z \max}$ (bottom) on the chamfer dimensions in z, Ch_{zz} , and in y, Ch_{zy} . The red point, at $(Ch_{zz}, Ch_{zy}) = (0.73, 0.26)$ mm was initially selected. Undulator tuning considerations prompted a change to the orange point at $(Ch_{zz}, Ch_{zy}) = (0.5, 0.2)$ mm.

3-D Design Work

The aspects of the design that must be done using 3-D codes are those that involve the roll-off of the on-axis field in the lateral (x) direction, the widths of the magnet and pole in x, and the chamfers at the x end of the magnet and pole.

The ‘good-field’ region in the undulator is ± 5 mm in x to allow for steering of the beam through the undulator and for beam displacements during injection. The roll-off is the peak-to-peak change of field over the range from -5 to +5 mm in the x direction, at the center of the pole in z. The limit on the field roll-off is set by requiring that the photon energies from electrons traveling within the ‘good-field’ region are the same as far as the user can tell, or specifically, to within 10% of the intrinsic width of the 3rd harmonic. (The roll-off is not used to limit the integrated multipole moments; those are separate requirements.) The full width at half maximum of the 3rd harmonic for a 4.8-m-long undulator is $\Delta E_{\gamma}/E_{\gamma} = 5.54 \cdot 10^{-3}$, and for a 2.4-m-long undulator it is $7.10 \cdot 10^{-3}$. These translate to $\Delta B/B = 0.0019$ or 0.0024 . For $B \sim 3460$ G, the roll-off limit becomes 6.6 to 8.3 G.

The width of the pole is limited by the need to fit around the vacuum chamber, with some allowance for clamping, so 44 mm is chosen, the same as many of the recent APS undulators. As with the magnet height, the on-

axis field keeps growing the wider the magnet. The limit on the width then becomes what fits with the existing vacuum chamber. Sixty-seven mm is chosen; at that width any gain from a wider magnet is diminishing anyway. The chamfers at the x edge of the magnet are entirely determined by engineering requirements for the clamping scheme and fitting around the vacuum chamber.

The chamfer on the x edge of the pole remains to be set. The surface plots in Fig. 4 show the effects of the x and y dimensions of the chamfer (Ch_{xx} and Ch_{xy} , respectively) on the effective undulator field (top) and on the field roll-off (bottom). As the x chamfer dimension becomes larger, the pole is effectively narrowed and the on-axis field grows. As the pole narrows, there is initially no effect on the roll-off, but then the roll-off begins to grow rapidly. The red dot marks the selected pole x chamfer dimensions (Ch_{xx}, Ch_{xy}) of (7, 4) mm. There is noise on the right side of the roll-off plot, probably due to a meshing issue, but since its level is ~ 1 G it was not pursued.

The production of the 17.2-mm-period undulator is now underway.

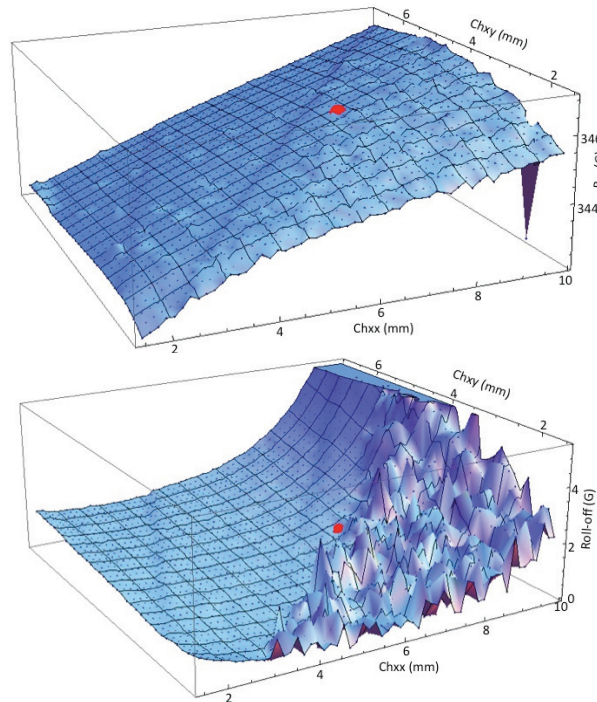


Figure 4: Surface plots showing the dependence of the effective field (top) and the field roll-off (bottom) on the chamfer dimensions in x, Ch_{xx} , and in y, Ch_{xy} . The red point, at $(Ch_{xx}, Ch_{xy}) = (7, 4)$ mm is the selected value.

REFERENCES

- [1] K. C. Harkay et al., “APS Superconducting Undulator Beam Commissioning Results,” WEOAA3, NA-PAC’13.
- [2] Opera Electromagnetics Finite Element Software Suite, Cobham Technical Services – Vector Fields Software.